

Microstructure and magnetorheology of graphite-based MR elastomers

T. F. Tian · W. H. Li · G. Alici · H. Du · Y. M. Deng

Received: 8 December 2010 / Revised: 8 May 2011 / Accepted: 6 June 2011 / Published online: 29 June 2011
© Springer-Verlag 2011

Abstract This study focuses on the magnetorheology of graphite-based magnetorheological elastomers (Gr MREs). By introducing graphite to conventional MREs, the Gr MREs with various graphite weight fractions are fabricated. Both steady-state and dynamic tests were conducted to study rheological properties of the samples. For dynamic tests, the effects of magnetic field, strain amplitude and frequency on both storage modulus and loss modulus were measured. The influence of graphite weight fraction on mechanical performances of these samples was summarized. Also, the microstructures of isotropic and anisotropic Gr MREs were observed. In anisotropic MREs, the graphite powders disperse in matrix randomly. The graphite particles lead to an increment of initial mechanical properties and a decrement of the MR effect.

Keywords Magnetorheological elastomers · Microstructure · Graphite · Magnetorheology

Introduction

Magnetorheological elastomers (MREs) are smart materials where polarized particles are suspended in a non-magnetic solid or gel-like matrix (Ginder et al. 2002). These materials exhibit characteristics that their moduli can be reversely controlled by an external magnetic field. MREs have recently found a variety of applications, such as adaptive tuned vibration absorbers, dampers, sensors and so on (Deng et al. 2006; Ni et al. 2009; Zhang and Li 2009; Kim et al. 2011; Xu et al. 2010; Zhang et al. 2010; Chen et al. 2007; Li et al. 2009; Bica 2010).

MREs generally consist of three major components: magnetizable particles, matrix and additives. Iron particles are generally used as the filler material to fabricate MREs; this is because iron has one of the highest saturation magnetisation values of metallic elements as well as high permeability, low remnant magnetisation and high saturation magnetisation. High permeability and saturation magnetisation are thought to provide high inter-particle attraction and thereby a high MR effect. The effect of particle shape, size and volume fraction on the overall MRE performances have been intensively investigated. Lokander and Stenberg (2003) measured the MR effect for isotropic nitrile rubber MRE with varying sizes and content of iron particles. The MR effect was larger for materials with ASC300 iron (particle size $<60\ \mu\text{m}$) than for materials with carbonyl iron (particle size $3.9\text{--}5.0\ \mu\text{m}$). Demchuk and Kuzmin (2002) studied the effect that the size of the filler particles on the shear storage modulus and loss modulus of isotropic and aligned MR elastomers. They found that without the field, the modulus for MRE with larger particles ($13\ \mu\text{m}$) was smaller than for fine

T. F. Tian · W. H. Li (✉) · G. Alici
School of Mechanical, Materials and Mechatronic
Engineering, University of Wollongong, Wollongong,
NSW 2522, Australia
e-mail: weihuali@uow.edu.au

H. Du
School of Electrical, Computer and Telecommunications
Engineering, University of Wollongong, Wollongong,
NSW 2522, Australia

Y. M. Deng
Faculty of Mechanical Engineering and Mechanics,
Ningbo University, Zhejiang Province 315211,
People's Republic of China

Table 1 Components of Gr MRE samples

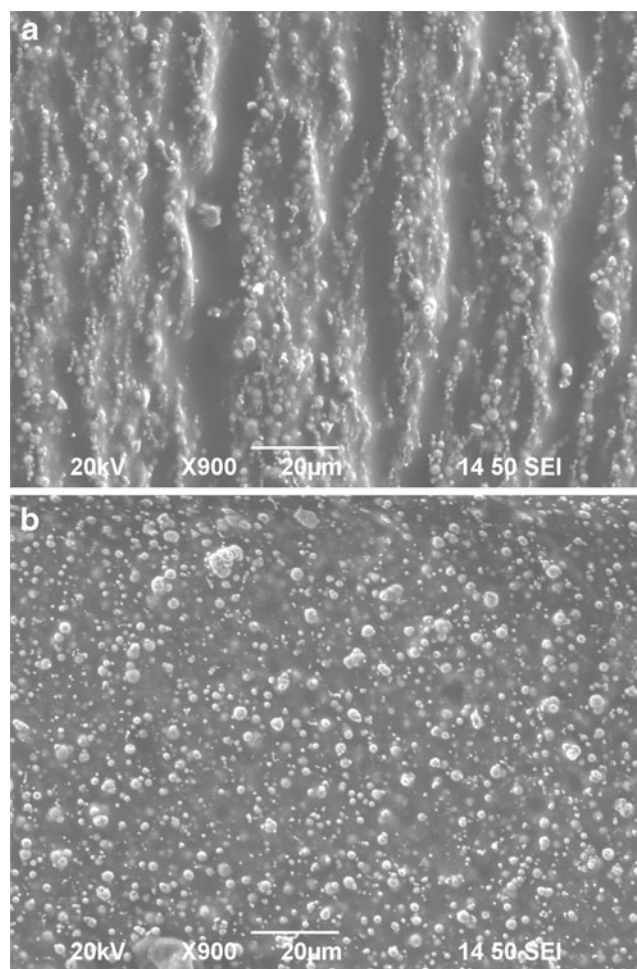
Sample no.	Graphite based MREs							
	1	2	3	4	5	6	7	8
Carbonyl iron	10 g	10 g	10 g	10 g	10 g	10 g	10 g	10 g
Silicone oil	3 g	3 g	3 g	3 g	3 g	3 g	3 g	3 g
Silicone rubber	3 g	3 g	3 g	3 g	3 g	3 g	3 g	3 g
Graphite	0 g	1 g	2 g	3 g	3.5 g	4 g	4.5 g	5 g
Graphite weight fraction (Gr %)	0%	5.88%	11.11%	15.79%	17.95%	20%	21.95%	23.81%

particles (3.5 μm). Under a magnetic field, the situation was reversed. The field strength increased the modulus of the MRE with larger particles exceeded the modulus of the MRE with fine particles significantly. The optimal particle volume fraction for the largest relative change in modulus at saturation was predicted to be 27% (Davis 1999). Shiga et al. (1995) measured the increase in shear modulus as a function of the particle volume fraction. For aligned MREs, the change in shear modulus increases with an increasing particle volume fraction. When the concentration of filler is higher than 30 vol.%, the mechanical properties of the composite deteriorate rapidly and the stiffening of the material is larger than the increase of the MR effect. Lokander and Stenberg (2003) measured the tensile strength of isotropic MR elastomers and found that the fracture stress as a function of the content of iron was almost constant when the iron contents were up to approximately 30% by volume. This optimal volume fraction was also extended to fabricate new MR elastomers with bimodal iron particles, where the two particles have sizes of 50 and 5 μm , respectively. The experimental results demonstrated that the bimodal particle-based MREs have enhanced MR effect (Li and Zhang 2010) compared with conventional MREs.

Both natural rubber and silicone rubber are used as typical matrixes (Gong et al. 2005). Natural rubber is an elastomer. The purified form of natural rubber is the chemical polyisoprene which can also be produced synthetically. Heat is normally required to vulcanise silicone rubber. The silicone rubber and a vulcanising silicon sealant (at room temperature) are mixed with silicon oil to changing its ductility. The silicon oil is selected on the basis of preliminary studies with different elastomers. Polydimethylsiloxanes (PDMS) is one example of silicon rubber. The PDMS have a low surface tension and are capable of wetting most surfaces. The stability and chemical neutrality of the system also enables the adhesive to bond to the metals (De Buyl 2001).

Additives are commonly used to adjust the mechanical and chemical properties or electrical performance of MR fluids (Park et al. 2009; Fang et al. 2009) as well as MR elastomers (Zhang et al. 2008). Silicone oil is

an additive to increase the gaps between the matrix molecules and to decrease the gaps between the conglutination of molecules. Apart from increasing the plasticity and fluidity of the matrix, the additives can average the distribution of internal stress in the materials, which makes them ideal for fabricating MRE materials (Leblanc 2002). Graphite powder is a kind of additive which can affect the magnetorheology and electrical conductivity of MREs (Li et al. 2009; Bica 2009; Zou et al. 2009). By introducing graphite microparticles into

**Fig. 1** Microstructure of Gr MREs (Gr 0%) **a** anisotropic **b** isotropic

the elastic matrix, MREs behave a lower electrical conductive characteristic, which has a potential to work as a sensing material for development of force and magnetic field sensors (Li et al. 2009). However, the study of magnetorheology of these materials is insufficient. In particular, a few reports are found to investigate the relationship between microstructures and the overall MR performances. This work aims to address this problem.

This paper is organized as follows. Followed by the Introduction, the fabrication of both isotropic and anisotropic MRE samples were described. The SEM images of these samples will be reported in Section “[Microstructure observation](#)”. Section “[Experimental setup and results steady-state and dynamic properties of MREs](#)” presents the characterization of both steady and dynamic properties of these samples. The main finding will be summarized in the conclusion section.

MRE fabrication

The materials used for the Graphite MR Elastomers are: silicone rubber (Selleys Pty. LTD); silicone oil, type 378364 (Sigma–Aldrich Pty. LTD); carbonyl iron particles, type C3518 (Sigma–Aldrich Pty. LTD) and graphite powder, type 282863 (Sigma–Aldrich Pty. LTD). The particle sizes of graphite powder are about 20 μm , while the iron particles’ diameter is between 3 and 5 μm at normal distribution.

In this study, both isotropic and anisotropic MRE samples with different graphite weight fractions (Gr wt.%) were fabricated. Table 1 shows the compositions of all graphite MRE samples. All the samples contain the same compositions of 10 g carbonyl iron particles, 3 g silicone rubber and 3 g silicone oil. The only difference is the graphite weight fraction, which is from 0% to 23.81%. For each composition, two samples, namely

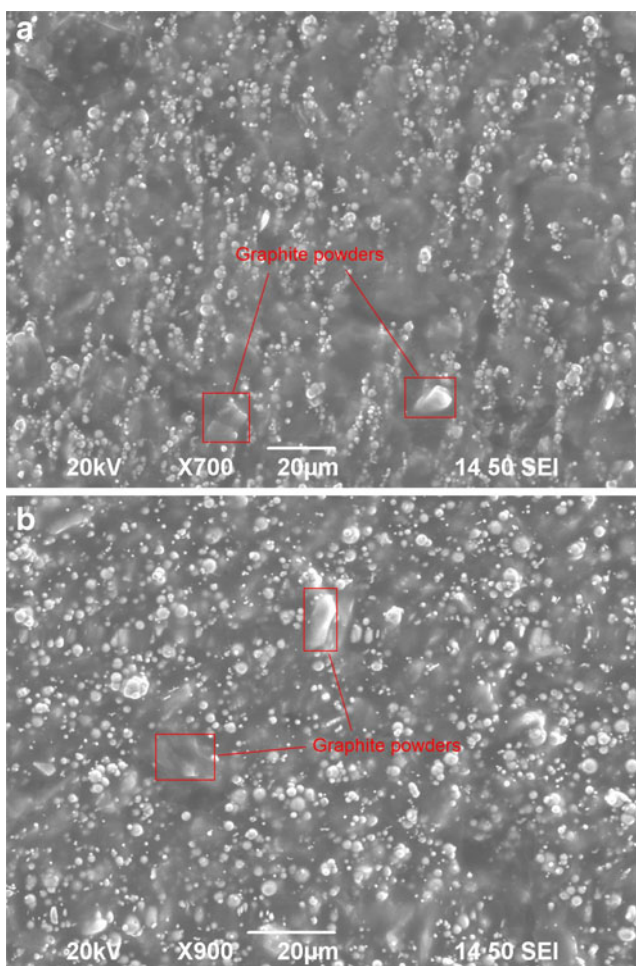


Fig. 2 Microstructure of Gr MREs (Gr 11.11%) **a** anisotropic **b** isotropic

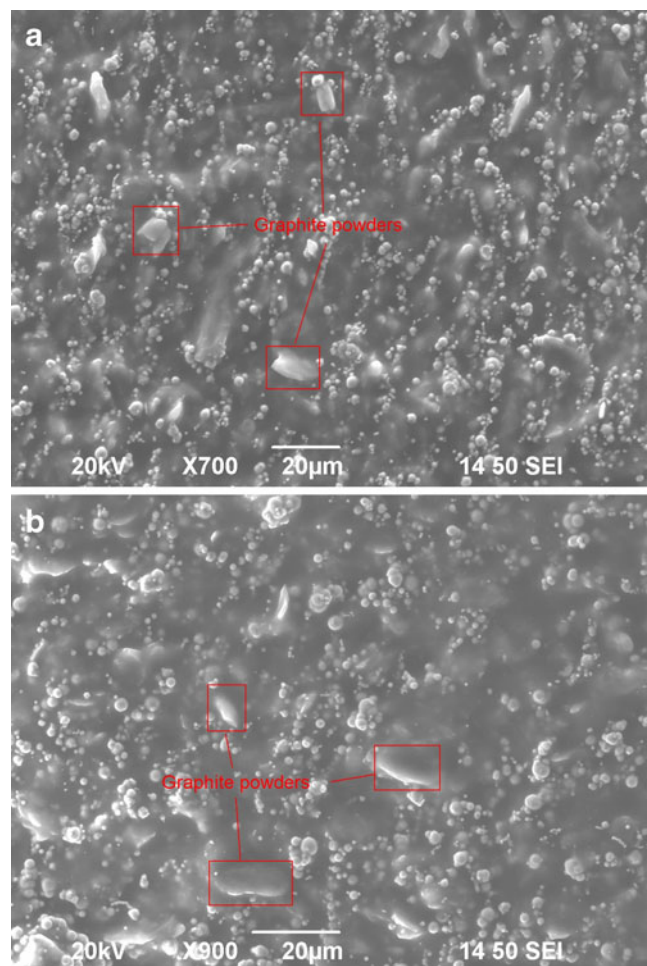


Fig. 3 Microstructure of Gr MREs (Gr 20%) **a** anisotropic **b** isotropic

isotropic and anisotropic, were fabricated for the study of magnetorheological and structural properties.

The general procedure for fabricating an anisotropic MR elastomer with natural rubber is similar to conventional rubber. Normally, the ingredients are natural rubber, zinc oxide, stearic acid, sulphur and iron particles. After all the ingredients are evenly mixed in a mixing machine at a high temperature such as 120°, the mixture is packed in a mould and then cured

under an magnetic field for a certain time. The samples are then left at the room temperature for more than 24 h prior to testing. The chain formation results from the anisotropic magnetic forces among the particles. The MREs fabricated with this method are called anisotropic MREs (Li et al. 2009). For isotropic MREs, carbonyl iron particles firstly immerse in silicone oil then were mixed with silicone rubber. All the ingredients in the beaker were mixed by using a stirrer

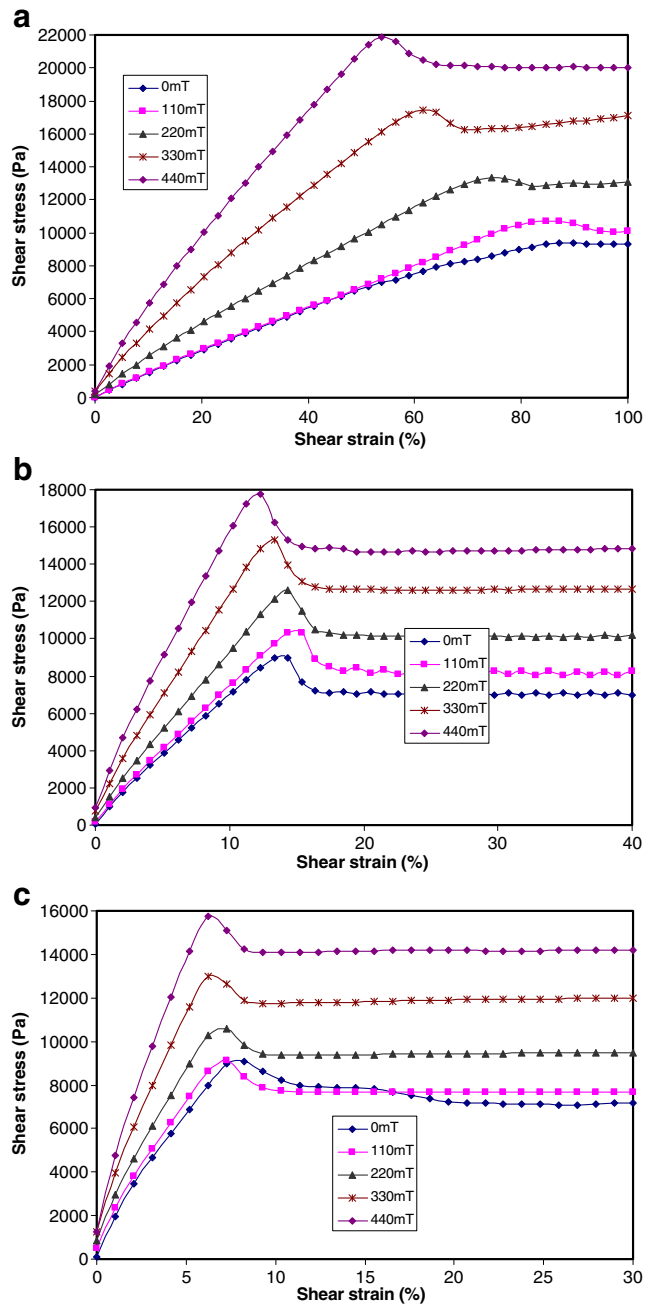


Fig. 4 Strain-stress curve versus magnetic field (isotropic MRE) **a** Gr 0% **b** 15.79% **c** Gr 23.81%

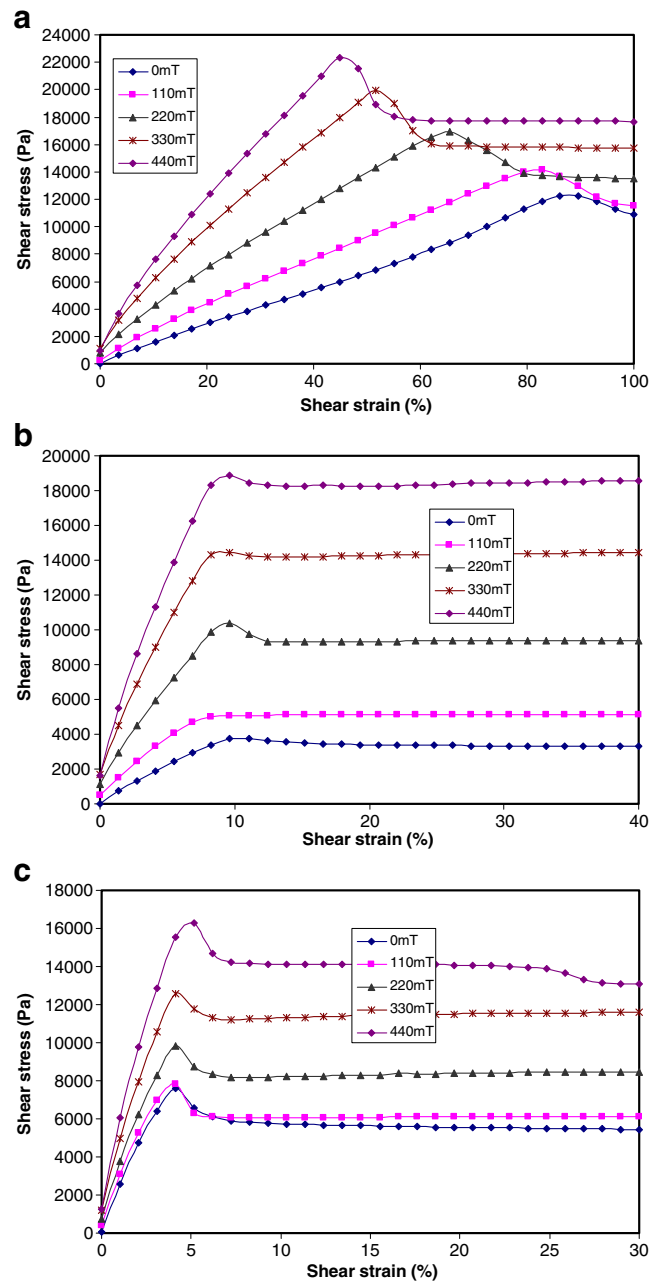


Fig. 5 Strain-stress curve versus magnetic field (anisotropic MRE) **a** Gr 0% **b** 15.79% **c** Gr 23.81%

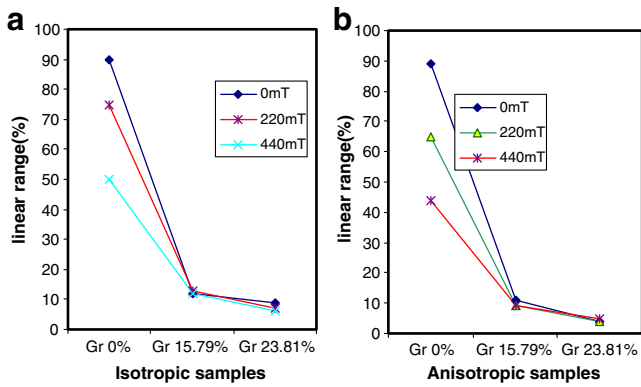


Fig. 6 Linear ranges versus different samples **a** isotropic samples **b** anisotropic samples

bar for about 5 min at room temperature. After all ingredients were evenly mixed, the mixture was put under a vacuum to remove air bubbles, and then cured for 24 h at room temperature in an open sheet mould without a magnetic field.

Microstructure observation

In this study, LV-SEM (JSM 6490LV SEM) was used to observe microstructures of MRE samples. Figures 1, 2 and 3 show the Surface imaging for MRE microstructures.

Figure 1a and b shows the microstructure of isotropic and anisotropic graphite MREs without graphite, respectively. The carbonyl iron particles array in chains in the anisotropic sample and disperse randomly in the isotropic sample. According to Figs. 2a and 3a, in the anisotropic Gr MREs, the carbonyl iron particles array in chains and the graphite powders disperse in the matrix randomly. The reason of this phenomenon is that the magnetic field only affects the carbonyl iron

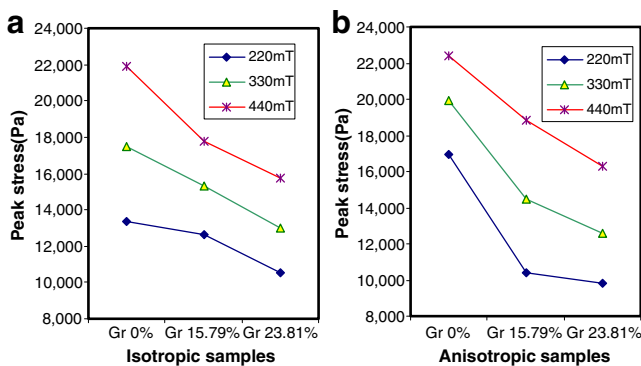


Fig. 7 Peaks stresses versus different samples **a** isotropic samples **b** anisotropic samples

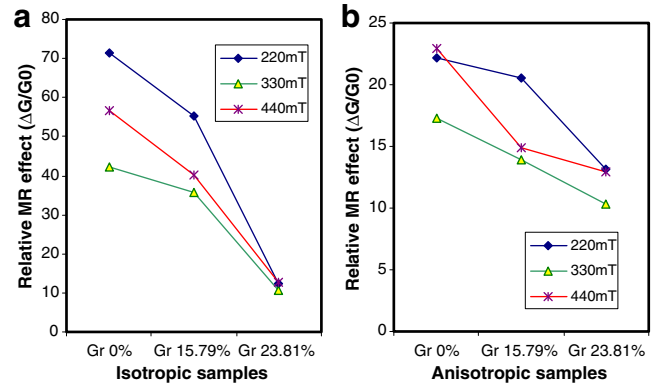


Fig. 8 Relative MR effects versus different samples **a** isotropic samples **b** anisotropic samples

particles, but not the graphite. So by the magnetism, the carbonyl iron particles move to chains along the same direction as the magnetic field in the matrix.

By compare Figs. 1a, 2a and 3a, we can see that the carbonyl iron chains in the sample without graphite have the best lines performance. Further, the carbonyl

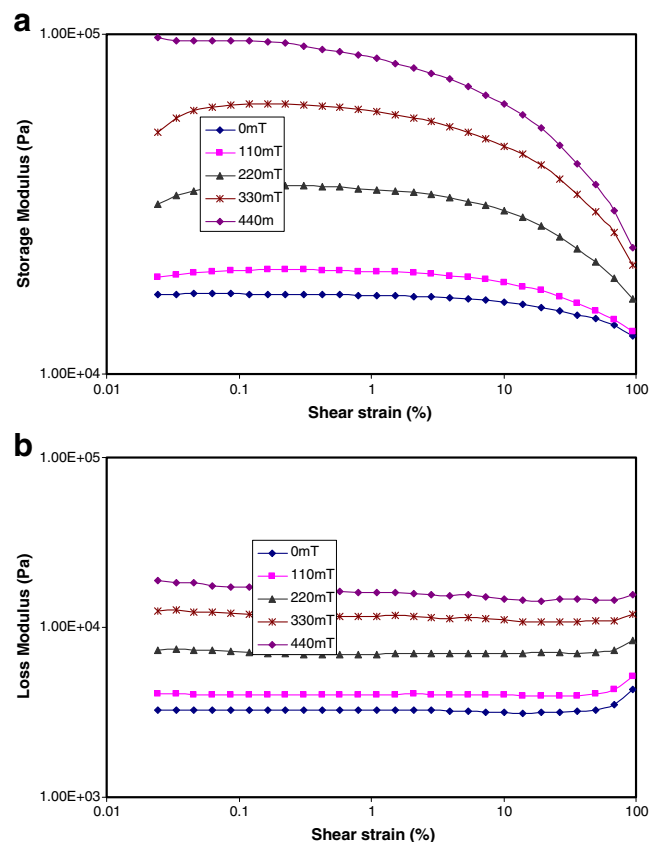


Fig. 9 Storage and Loss Modulus versus strain amplitude sweep (isotropic MRE Gr 0%) **a** Storage modulus vs. shear strain **b** Loss modulus vs. shear strain

iron chains in Fig. 2a are aligned better than those in Fig. 3a. The reason is that when the mixture of carbonyl iron, silicone rubber, silicone oil and graphite is curing under the magnetic field, the graphite powders in graphite MREs affect the carbonyl iron particles' movement. The more graphite in the mixture, the more effects are applied on to the carbonyl iron chains, which influence the magnetorheology of MREs.

Experimental setup and results steady-state and dynamic properties of MREs

Experimental device

A rotational Rheometer (MCR 301, Anton Paar Companies, Germany) and a Magneto Rheological Device (MRD 180, Anton Paar Companies, Germany) were used to measure the MREs' mechanical properties. The Magneto Rheological Device is equipped with an electromagnetic kit which can generate a magnetic field perpendicular to the direction of the shear flow. A 20-mm diameter parallel-plate measuring system with

1 mm gap was used. The samples were sandwiched between a rotary disk and a base parallel. In this study, a steady-state rotary shear and oscillatory shear were both used for the experiments.

In this experiment, the magnetic flux density of the sample of MRE (B_{MRE}) in the measuring gap depends not only on the current (I) applied to the samples and the magnetic properties of MRE materials. As the permeability of MRE samples varies little, an empirical equation, $B_{\text{MRE}} = 220 I$, was employed to predict the flux density for different MRE samples, where the units of B_{MRE} and I are in mT and amp (A), respectively.

In the following test, the test current varies from 0 to 2 A with the increment 0.5 A, whose intensity of magnetic field is 0 to 440 mT with the increment 110 mT.

Steady state

Under rotary shear the shear stress and shear strain of MREs under fields varying from 0~440 mT were measured at room temperature and 5 rad/s angular

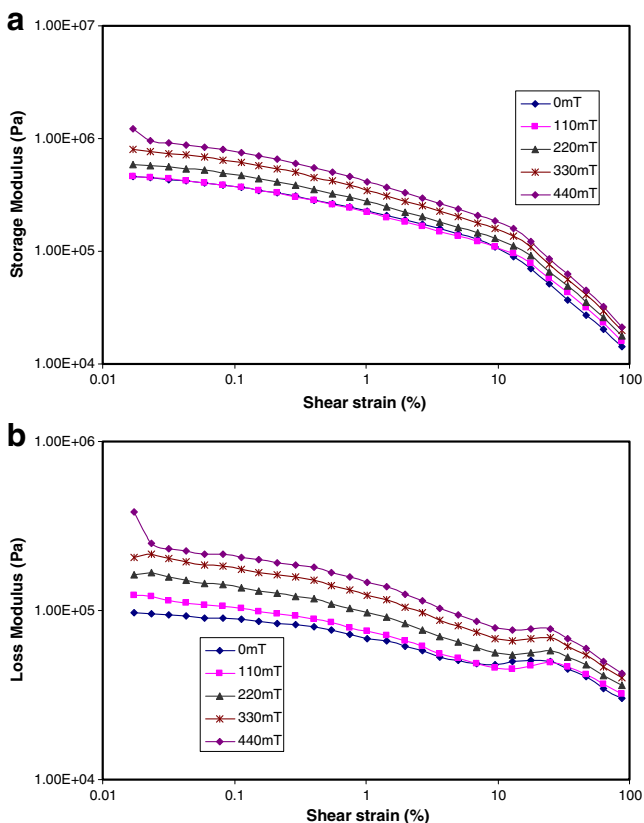


Fig. 10 Storage and Loss Modulus versus strain amplitude sweep (isotropic MRE Gr 20%) **a** Storage modulus vs. shear strain **b** Loss modulus vs. shear strain

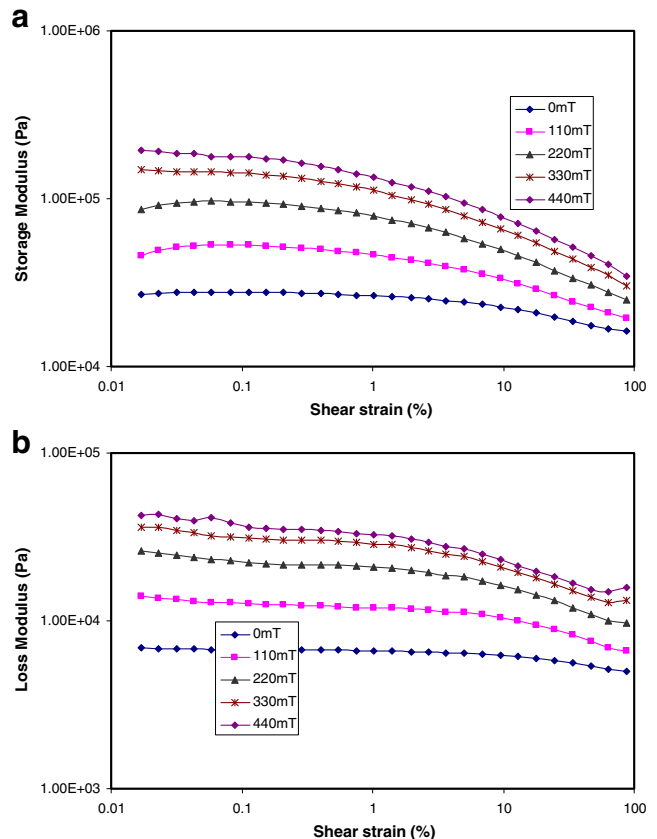


Fig. 11 Storage and Loss Modulus versus strain amplitude sweep (anisotropic MRE Gr 0%) **a** Storage modulus vs. shear strain **b** Loss modulus vs. shear strain

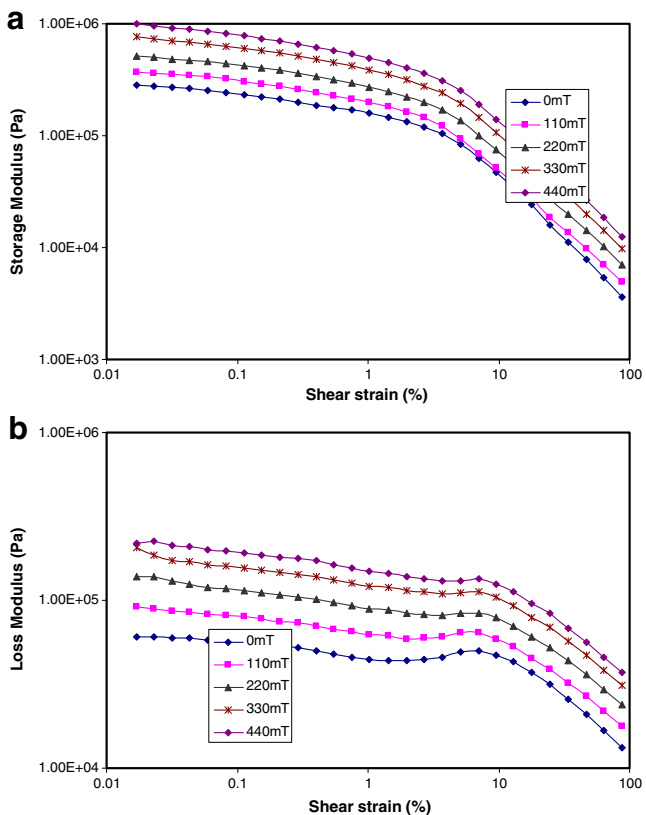


Fig. 12 Storage and Loss Modulus versus strain amplitude sweep (anisotropic MRE Gr 20%) **a** Storage modulus vs. shear strain **b** Loss modulus vs. shear strain

frequency. The shear rate range is from 0.0005 to 5. The MR effect was evaluated by measuring the shear strain–stress curve of the sample with and without a magnetic field applied.

Figures 4a–c and 5a–c show the strain–stress curve of different samples at five different magnetic field intensities ranging from 0 to 440 mT. The slope of the strain–stress curve is the shear modulus of the material.

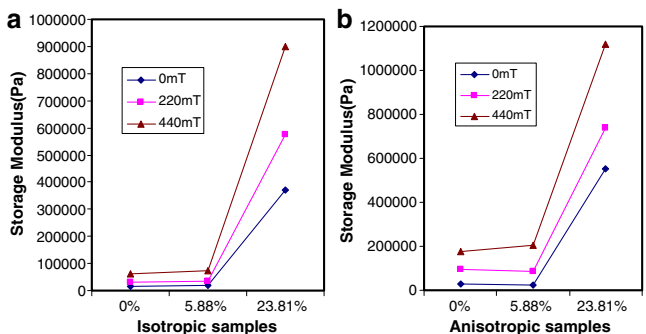


Fig. 13 Storage Modulus of different samples at 10% shear strain **a** isotropic samples **b** anisotropic samples

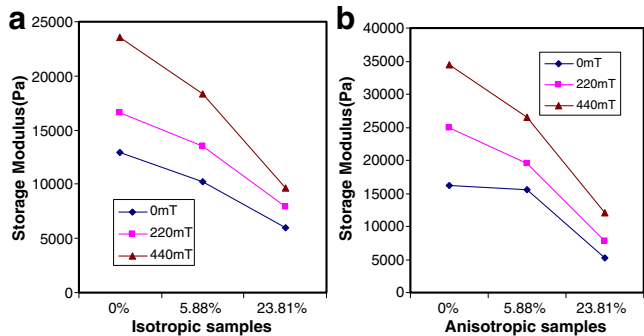


Fig. 14 Storage Modulus of different samples at 87.5% shear strain **a** isotropic samples **b** anisotropic samples

As can be seen in the figures, all the samples’ shear modulus show an increasing trend with magnetic field before they reach magnetic saturation at high field strength, which proves that all the MRE samples exhibit obvious MR effects. In Fig. 4c, we can see that the curve at 0 mT, which is the zero-field modulus

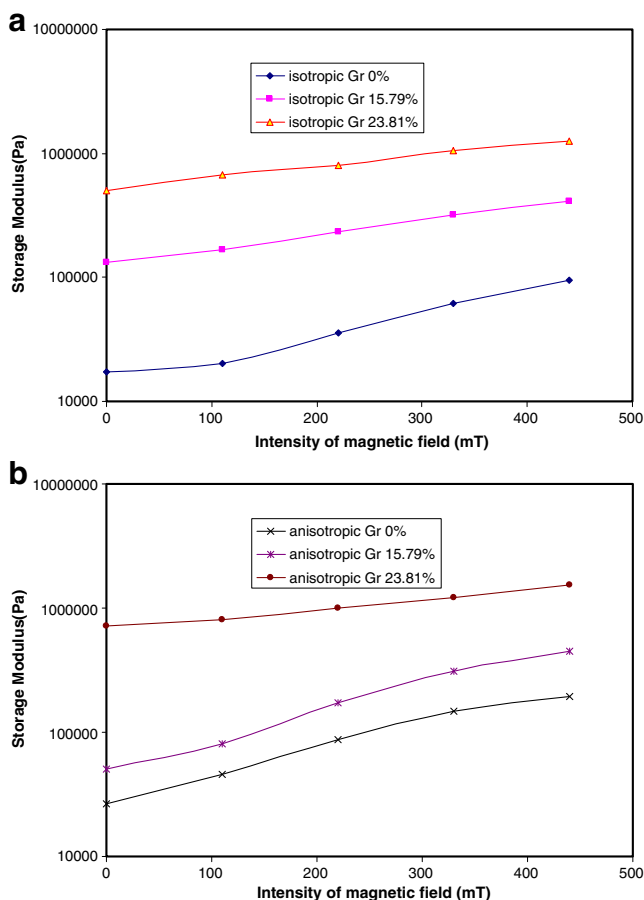


Fig. 15 Storage Modulus versus magnetic field at 0.1% shear strain **a** isotropic samples **b** anisotropic samples

of the 23.81 wt.% isotropic sample, shows a higher zero-field modulus compared with the lower graphite concentration samples.

Also from Figs. 4 and 5, the shear stress shows a linear relationship with the shear strain when the strain is within a range. This means the MRE acts with linear viscoelastic properties when the strain is below a limitation. For conventional MREs, the limitation is around 50% shear strain (Li et al. 2010), which was much higher than that of MR fluids (Li et al. 2002, 2003). When the graphite weight fraction increases from 0% to 15.79%, the range of linearity decreases from 50% to around 10%. For the samples with higher graphite weight fraction as 23.81%, the linearity ranges are only 6% and 4% for isotropic and anisotropic samples, respectively. When the strain is above the limitation, the shear stress reaches a saturation (maximum value) and decrease steadily. This might be due to the sliding effect. Additionally, other factors, such as the sample surface roughness and the normal force, could contribute to the resultant stress. In particular,

they influence the static friction between the MRE sample and the upper plate, which consequently result in overshoots, as shown in Figs. 4 and 5.

Figure 6 summarized the linear ranges of different samples at various magnetic field intensities. For the isotropic and anisotropic samples with same compositions, the isotropic samples always have the bigger linearity ranges and steady shear stress than those of anisotropic samples except for the data at 0 mT magnetic field because that without applied magnetic field, the isotropic and anisotropic samples show similar linearity ranges.

For each curve, the slope equals to the ratio of peak shear stress to the relevant shear strain. By analyzing the slope and of the curves, it is easy to see that the more graphite in the material, the less growth of slopes when the magnetic field increase from 0 to 440 mT. This is because of the contributions of graphite powders to the stiffness of the samples. The graphite increases the initial stiffness of graphite MREs; thus, the stiffness change from the MR effect cannot be as the same as the conventional MREs. Figure 7 shows the peaks stresses

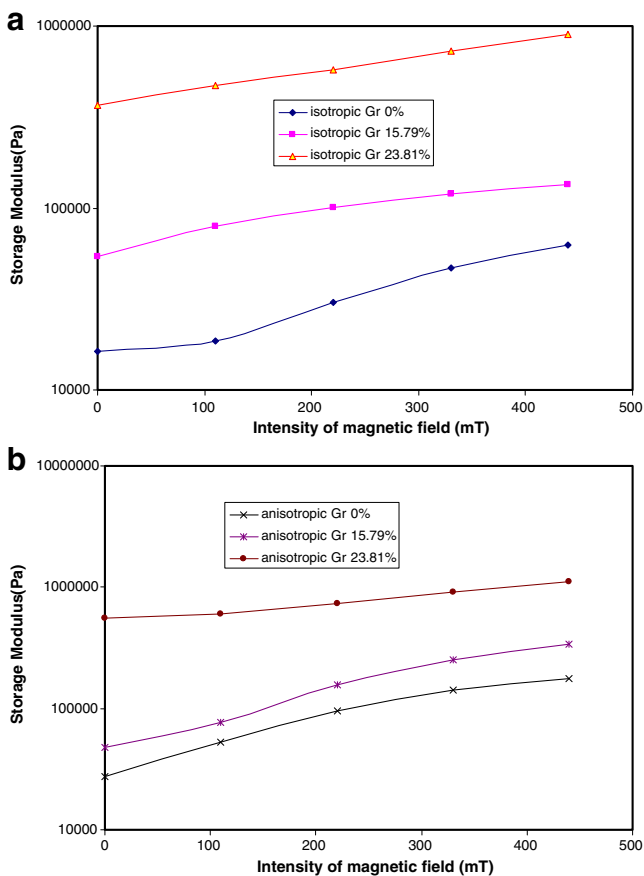


Fig. 16 Storage Modulus versus magnetic field at 10% shear strain **a** isotropic samples **b** anisotropic samples

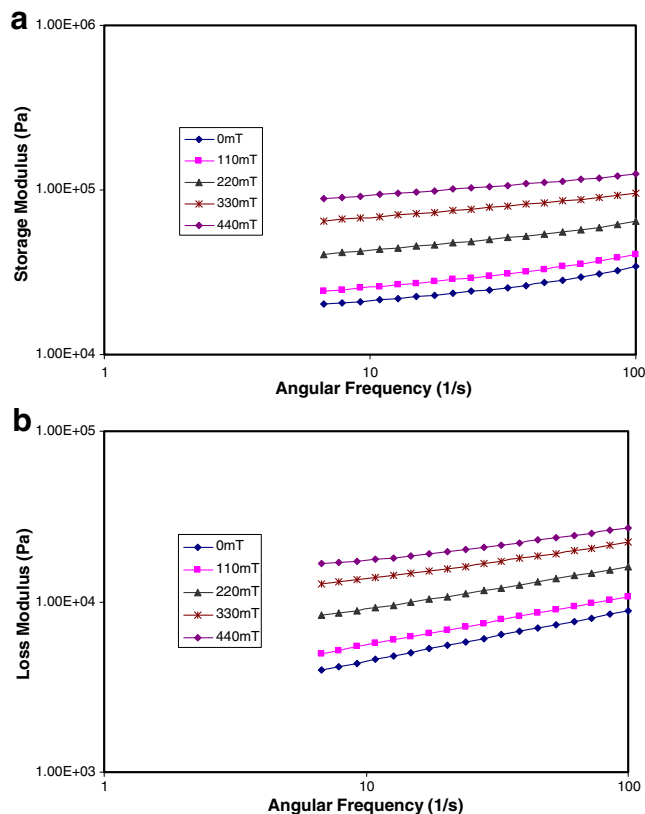


Fig. 17 Storage and Loss Modulus versus angular frequency sweep (isotropic MRE Gr 0%) **a** Storage modulus vs. shear strain **b** Loss modulus vs. shear strain

of different samples at 220, 330 and 440 mT magnetic field.

The relative MR effect ($\Delta G_{\max}/G_0$) of these samples is shown in Fig. 8. Here, G_0 denotes the MRE samples' zero-field modulus, ΔG_{\max} denotes the saturated field-induced modulus, and $\Delta G_{\max}/G_0$ denotes the relative MR effect. It can be seen from Fig. 8 that G_0 is enhanced with the increase in graphite powders content. This result indicates that graphite powders can modify particle properties and, consequently, influenced the MR effect. The MR effects correspond well with the microstructures of graphite MREs.

Dynamic tests result

In order to obtain the dynamic mechanical behaviour of MRE, both angular frequency sweep tests and strain amplitude sweep tests were used. Five sets of data were collected for different amplitudes of oscillation, according to the various magnetic field inputs to the samples of MR elastomers. Same as the steady state tests, five different magnetic field intensities, 0, 110,

220, 330 and 440 mT, were used in this experiment. The amplitude of shear strain in angular frequency sweep tests is set at 1% and the input frequency was 5 Hz in the strain amplitude sweep tests.

Strain amplitude sweep

In the strain sweep test, the storage and loss moduli were tested by varying strain from 0.01% to 100% at different magnetic fields and room temperature. Figures 9, 10, 11 and 12 show the changing of storage modulus and loss moduli at the strain amplitude sweep.

In Figs. 9, 10, 11 and 12, the overall trend of storage modulus is decreasing with the strain amplitude. It goes down smoothly within 10% shear strain and begins to drop significantly over 10% shear strain, with which we can say that within 10% shear strain, the storage modulus and loss modulus both show approximately a linear relationship with the shear strain. Except for isotropic MREs without graphite, the Loss modulus has almost the same trend of storage modulus. This means

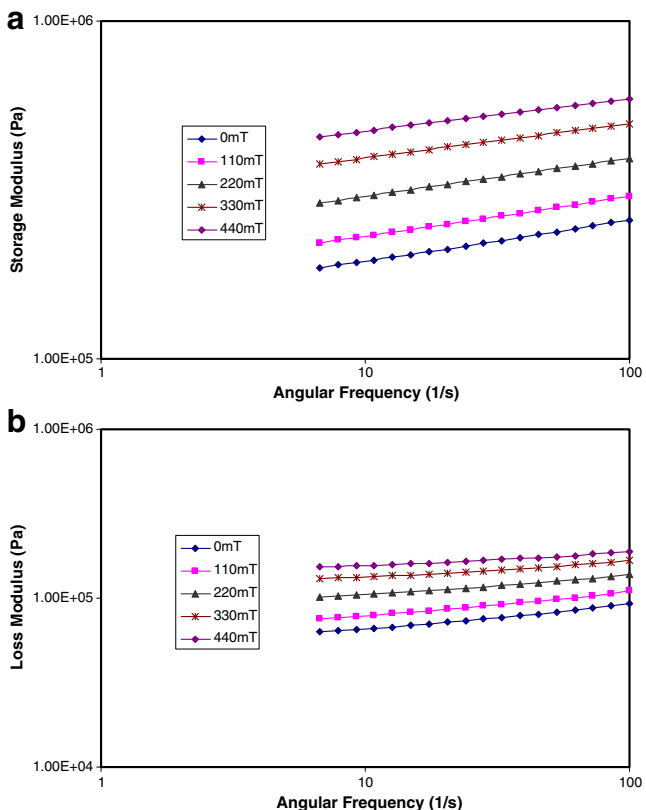


Fig. 18 Storage and Loss Modulus versus angular frequency sweep (isotropic MRE Gr 20%) **a** Storage modulus vs. shear strain **b** Loss modulus vs. shear strain

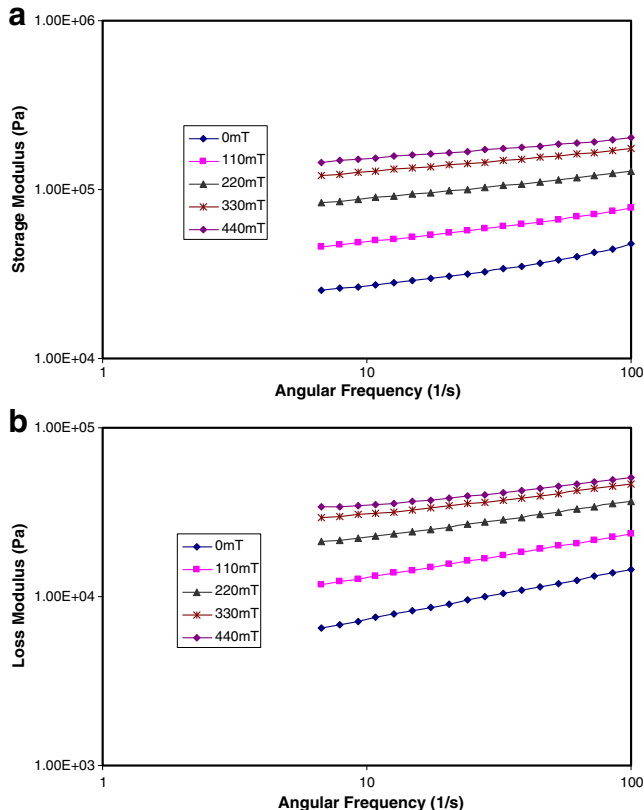


Fig. 19 Storage and Loss Modulus versus angular frequency sweep (anisotropic MRE Gr 0%) **a** Storage modulus vs. shear strain **b** Loss modulus vs. shear strain

at the high shear strain, the storage and loss moduli are much smaller than that at low shear strain.

Figures 13 and 14 shows the storage modulus of different samples at 0, 220 and 440 mT magnetic field. The data are collected at 10% and 87.5% shear strain, respectively. As can be seen in Fig. 13, the storage modulus of all samples shows an increasing trend with graphite weight fraction at 10% shear strain which is in the linear range for most of samples. In Fig. 14, it turns to a diminishing trend with graphite weight fraction at 87.5% shear strain which is out of the linear range. This means in the linear range of shear strain, the samples with higher graphite weight fraction have the bigger storage modulus.

Figures 15 and 16 show the storage modulus versus magnetic field at 0.1% and 10% shear strain, respectively. The two shear strains are the beginning and end of linear range.

In Figs. 15 and 16 we can see that the storage modulus shows an increasing trend with the intensity of magnetic field. The ratio of storage modulus at 440 mT to that at 0 mT is the MR effect. The MR effect of

isotropic MREs with 0% graphite is around 4.5, when the graphite weight fraction increases to 15.79% and 23.81%, the MR effect decreases to around 2.8 and 2.8, respectively, which are all a little bigger than those in the angular frequency sweep. For anisotropic samples, the MR effects of 0%, 20% and 23.81% Gr MREs are 4.8, 3.2 and 2.2, respectively. This proves that again, with the growth of graphite weight fraction, the MR effect decreases.

Angular frequency sweep

In this test, the strain is set at 1%. According to the experimental equipments, the angular frequency was varied from 6 to 100 1/s at different magnetic fields of 0, 110, 220, 330 and 440 mT. The Figs. 17, 18, 19, and 20 show the storage and loss moduli curves of the MRE samples at frequency sweep and room temperature.

From the figures above, we can see that in the log–log scale, the storage and loss moduli of all the samples are both increasing linearly with the growth of

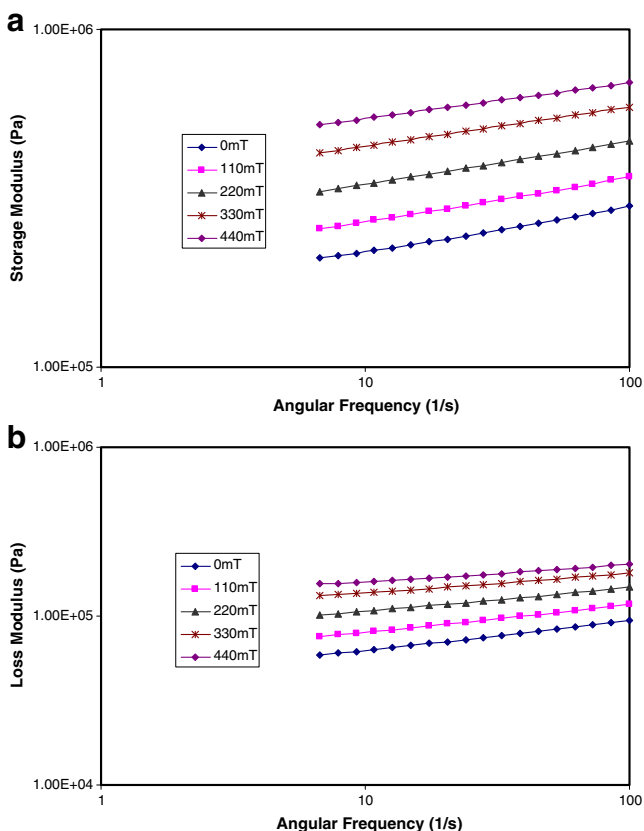


Fig. 20 Storage and Loss Modulus versus angular frequency sweep (anisotropic MRE Gr 20%) **a** Storage modulus vs. shear strain **b** Loss modulus vs. shear strain

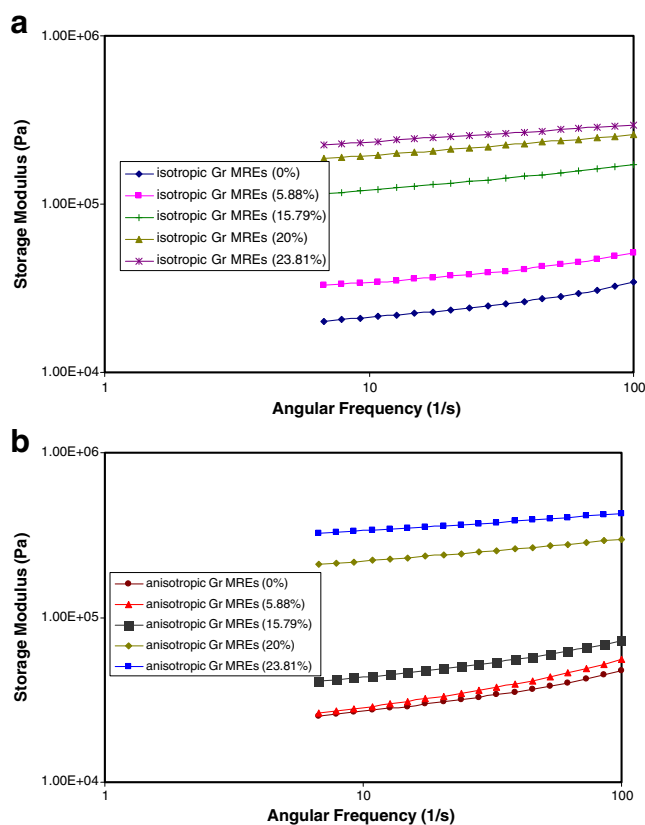


Fig. 21 Storage Modulus versus angular frequency sweep (without magnetic field) **a** isotropic **b** anisotropic

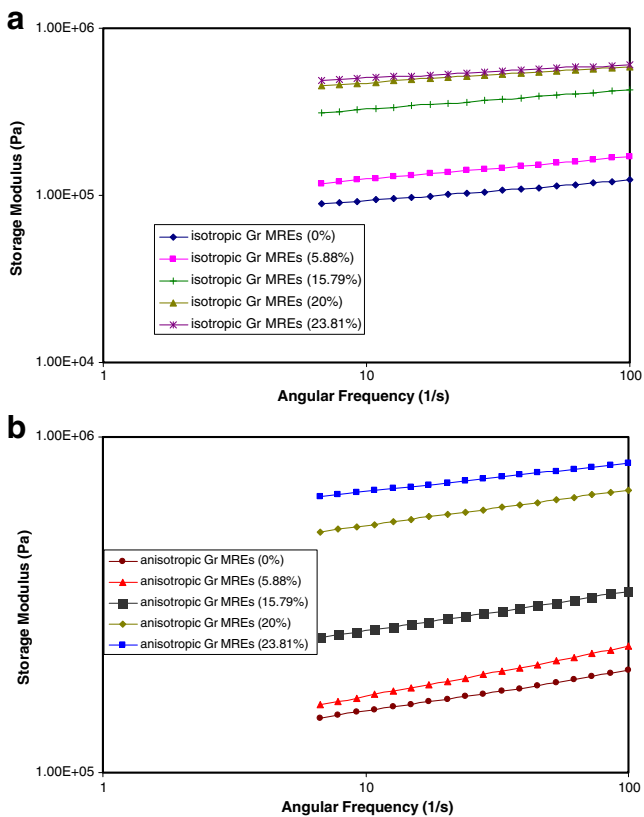


Fig. 22 Storage Modulus versus angular frequency sweep (with 440 mT magnetic field) **a** isotropic **b** anisotropic

angular frequency. This means that at a higher angular frequency, the samples have bigger storage and loss moduli. This logarithmically linear relationship of the storage and loss moduli to the angular frequency can be used to predict the storage and loss moduli at a certain frequency. The effect of the graphite weight fraction on the MR effect was shown in Figs. 21 and 22. It can be seen from these figures that with higher graphite weight fraction, the samples have a bigger storage modulus. This also proves that the graphite powder contributes to the initial stiffness of MRE samples.

The ratio of storage modulus at 440 mT to the storage modulus at 0 mT is the MR effect. The ratio of isotropic conventional MREs is around 4, when the graphite weight fraction increases to 15.79% and 23.81%, the MR effect are around 2.6 and 2.1, respectively. For anisotropic samples, the MR effects of conventional MREs, 20% and 23.81% Gr MREs are 5.2, 2.4 and 2.0, respectively. This means with the growth of graphite weight fraction, the MR effect decreases. This phenomenon is caused by the contribution of graphite powder to the samples' stiffness, because of which, the MR effect can only have less effects on the Gr MRE samples than conventional MREs.

Conclusion

Both isotropic and anisotropic Gr MREs with various graphite weight fractions were fabricated in this study. LA SEM was used to observe their microstructures. This observation shows that the graphite powders effect the forming of carbonyl iron chains. The sample with less graphite shows better-aligned carbonyl iron chains which affects the magnetorheology of MREs. Also by connecting two iron chains in parallel and connecting the disconnected iron chains the graphite contributes to the conductivity of MREs.

The steady state and dynamic tests such as strain amplitude sweep and angular frequency sweep were used to test the magnetorheology of Gr MREs. With the help of graphite in MREs, the Storage and Loss Moduli are both changed. The steady state tests showed that the graphite decreases or even diminish the viscoelastic linear range of MREs. The dynamic test proved that the samples with higher graphite weight fraction show higher initial storage and loss moduli and lower MR effects. The effect of graphite on the sensing capabilities of MR elastomers will be reported somewhere else.

Acknowledgements This project is supported by University of Wollongong through a UIC grant.

References

- Bica I (2009) Influence of the transverse magnetic field intensity upon the electric resistance of the magnetorheological elastomer containing graphite microparticles. *Mater Lett* 63(26):2230–2232
- Bica I (2010) Influence of the magnetic field on the electric conductivity of magnetorheological elastomers. *J Ind Eng Chem* 16(3):359–363
- Chen L, Gong XL, Li WH (2007) Microstructure and viscoelastic properties of anisotropic magnetorheological elastomers. *Smart Mater Struct* 16(6):2645–2650
- Davis LC (1999) Model of magnetorheological elastomers. *J Appl Phys* 85(6):3348–3351
- De Buyl F (2001) Silicone sealants and structural adhesives. *Int J Adhes Adhes* 21:411–422
- Demchuk SA, Kuzmin VA (2002) Viscoelastic properties of magnetorheological elastomers in the regime of dynamic deformation. *J Eng Phys Thermophys* 75(2):396–400
- Deng HX, Gong XL, Wang LH (2006) Development of an adaptive tuned vibration absorber with magnetorheological elastomer. *Smart Mater Struct* 15(5):N111–N116
- Fang FF, Choi HJ, Jhon MS (2009) Magnetorheology of soft magnetic carbonyl iron suspension with single-walled carbon nanotube additive and its yield stress scaling function. *Colloids Surf A* 351:46–51
- Ginder JM, Clark SM, Schlotter WF, Nichols ME (2002) Magnetostrictive phenomena in magnetorheological elastomers. *Int J Mod Phys B* 16(17&18):2412–2418

- Gong XL, Zhang XZ, Zhang PQ (2005) Fabrication and characterization of isotropic magnetorheological elastomers. *Polym Test* 24(5):669–676
- Kim YK, Koo JH, Kim KS, Kim SH (2011) Suppressing harmonic vibrations of a miniature cryogenic cooler using an adaptive tunable vibration absorber based on MR elastomers. *Rev Sci Instrum* 82:035103
- Leblanc JL (2002) Rubber-filler interactions and rheological properties in filled compounds. *Prog Polym Sci* 27(4):627–687
- Li WH, Zhang XZ (2010) A study of the magnetorheological effect of bimodal particle based magnetorheological elastomers. *Smart Mater Struct* 19(3):035002
- Li WH, Du H, Chen G, Yeo SH, Guo NQ (2002) Nonlinear rheological behavior of MR fluids: step strain experiments. *Smart Mater Struct* 11:209–217
- Li WH, Du H, Chen G, Yeo SH, Guo NQ (2003) Nonlinear viscoelastic properties of MR fluids under large-amplitude oscillatory shear. *Rheol Acta* 42:280–286
- Li WH, Kostidis K, Zhang XZ, Zhou Y (2009) Development of a force sensor working with MR Elastomers. In: 2009 Ieee/Asme International Conference on Advanced Intelligent Mechatronics, vols 1-3. ISBN: 978-1-4244-2853-3, pp 233–238
- Li WH, Zhou Y, Tian TF (2010) Viscoelastic properties of MR elastomers under harmonic loading. *Rheol Acta* 49:733–740
- Lokander M, Stenberg B (2003) Performance of isotropic magnetorheological rubber materials. *Polym Test* 22(3):245–251
- Ni ZC, Gong XL, Li JF, Chen L (2009) Study on a dynamic stiffness-tuning absorber with squeeze-strain enhanced magnetorheological elastomer. *J Intell Mater Syst Struct* 20(10):1195–1202
- Park BJ, Song KH, Choi HJ (2009) Magnetic carbonyl iron nanoparticle based magnetorheological suspension and its characteristics. *Mater Lett* 63:1350–1352
- Shiga T, Okada A, Kurauchi T (1995) Magnetorheological behaviour of composite gels. *J Appl Polym Sci* 58:787–792
- Xu ZB, Gong XL, Liao GJ, Chen XM (2010) An active-damping-compensated magnetorheological elastomer adaptive tuned vibration absorber. *J Intell Mater Syst Struct* 21(10):1039–1047
- Zhang XZ, Li WH (2009) Adaptive tuned dynamic vibration absorbers working with MR elastomers. *Smart Struct Syst* 5(5):517–529
- Zhang XZ, Peng SL, Wen WJ, Li WH (2008) Analysis and fabrication of patterned magnetorheological elastomers. *Smart Mater Struct* 17(4):045001
- Zhang W, Gong XL, Jiang WQ, Fan YC (2010) Investigation of the durability of anisotropic magnetorheological elastomers based on mixed rubber. *Smart Mater Struct* 19:085008
- Zou H, Zhang LQ, Tian M, Wu SZ, Zhao SH (2009) Study on the structure and properties of conductive silicone rubber filled with nickel-coated graphite. *J Appl Polym Sci* 115(5):2710–2717